THE JOURNAL OF BIOLOGICAL CHEMISTRY VOL. 281, NO. 20, pp. 13999–14008, May 19, 2006

Sequence-specific Interactions of Nascent *Escherichia coli* Polypeptides with Trigger Factor and Signal Recognition Particle*

Received for publication, January 23, 2006 Published, JBC Papers in Press, March 21, 2006, DOI 10.1074/jbc.M600638200

Ronald S. Ullers[‡1], Edith N. G. Houben[‡2], Josef Brunner[§], Bauke Oudega[‡], Nellie Harms[‡], and Joen Luirink[‡3]

From the [‡]Department of Molecular Microbiology, Institute of Molecular Cell Biology, Vrije Universiteit, 1081 HV Amsterdam, The Netherlands and [§]Institute of Biochemistry, Eidgenössische Technische Hochschule Zürich, CH-8093 Zürich, Switzerland

As nascent polypeptides exit the ribosomal tunnel they immediately associate with chaperones, folding catalysts, and targeting factors. These interactions are decisive for the future conformation and destination of the protein that is being synthesized. Using *Escherichia coli* as a model organism, we have systematically analyzed how the earliest contacts of nascent polypeptides with cytosolic factors depend on the nature and future destination of the emerging sequence using a photo cross-linking approach. Together, the data suggest that the chaperone trigger factor is adjacent to emerging sequences by default, consistent with both its placement near the nascent chain exit site and its cellular abundance. The signal recognition particle (SRP) effectively competes the contact with TF when a signal anchor (SA) sequence of a nascent inner membrane protein appears outside the ribosome. The SRP remains in contact with the SA and downstream sequences during further synthesis of ~30 amino acids. The contact with trigger factor is then restored unless another transmembrane segment reinitiates SRP binding. Importantly and in contrast to published data, the SRP appears perfectly capable of distinguishing SA sequences from signal sequences in secretory proteins at this early stage in biogenesis.

Synthesis of proteins takes place on ribosomes that appear to be functionally and structurally similar in pro- and eukaryotes. One of the key characteristics of the ribosome is a narrow cavity that is thought to conduct the nascent polypeptide from the peptidyl transferase center (PTC)[4] to the ribosomal surface. Crystal structures of the large ribosomal subunit have revealed that this "exit tunnel" is 100 Å long and only 15 Å in diameter, which would preclude extensive folding of the nascent peptide in the tunnel (1, 2). However, there is increasing evidence that the tunnel dynamically responds to the progressing polypeptide to allow partial folding (reviewed in Ref. 3).

At the ribosomal surface near the large ribosomal subunit L23, the nascent chain appears in the cytosol. At this stage, important decisions have to be made with respect to the future conformation and destination of the protein. Folding catalysts, chaperones, and targeting factors interact with the nascent polypeptide to avoid misfolding, aggregation, and erroneous sorting (4–7).

In vitro, trigger factor (TF) has been identified as the first chaperone in line to interact generically with nascent polypeptides in *Escherichia coli*. TF binds to ribosomes in a 1:1 stoichiometry (8) and was found to cross-link a variety of nascent chains derived from proteins of different origin (reviewed in Ref. 7). Although TF exhibits peptidyl-prolyl isomerase activity *in vitro* (9), the *in vivo* relevance of this activity remains unclear (10, 11). *In vivo*, TF displays functional overlap with the DnaK/J, GroEL/ES, and SecB chaperones that normally interact with longer nascent chains (10, 12–15). TF uses L23 as a ribosome attachment site, and this interaction appears crucial for the association of TF with nascent chains (16). Recent structural studies indicate that L23-bound TF arches over the exit of the ribosomal tunnel, creating a shielded "chamber" that may offer a protected environment for co-translational folding of protein domains (17).

The signal recognition particle (SRP) (reviewed in Ref. 7) specifically binds to hydrophobic targeting signals in nascent polypeptides. In *E. coli*, the SRP consist of two core subunits, the 48-kDa subunit Ffh (for fifty-four homologue) and 4.5 S RNA, which are homologous to the eukaryotic SRP54 and the 7 S RNA, respectively. Together with its receptor, FtsY, the SRP mediates targeting to the Sec-YidC complex in the inner membrane where insertion takes place in a co-translational process. The *E. coli* SRP predominantly targets nascent inner membrane proteins (IMPs) that are contacted at an early stage in their biosynthesis when the signal anchor (SA) sequence is not even fully exposed outside the ribosome (18–22). Noticeably, the SRP also uses L23 as a conserved attachment site on the ribosome (21, 23–25). *In vitro* binding and cross-link studies suggest that TF and SRP are able to bind simultaneously to one ribosome (26, 27), although they may influence each other's association with L23 (21). It remains elusive how *in vivo* binding of TF and SRP to the ribosome is regulated and how they orient themselves toward the nascent chain exit site in response to each other, the emerging polypeptide, and other cellular factors such as FtsY (26, 27). The recent cryo-electron microscopy structure of the eukaryotic SRP-ribosome-nascent chain complex suggests several contacts of SRP54 at and near L23 on the ribosome (28). Assuming that *E. coli* Ffh exhibits a similar structure and association with the ribosome, conformational changes appear required to avoid steric conflicts with TF (29).

In the present study, we have used an unbiased site-specific photo cross-linking approach to investigate the molecular contacts of short nascent polypeptides of different nature and destination. Together, the data suggest a default interaction of nascent chains with TF near the exit site at L23 irrespective of the length and nature of the polypeptide. SRP specifically interacts with nascent IMPs. Optimal contact with the SA sequence occurred at ~50–70 amino acids from the PTC with a sharp

* The costs of publication of this article were defrayed in part by the payment of page charges. This article must therefore be hereby marked "*advertisement*" in accordance with 18 U.S.C. Section 1734 solely to indicate this fact.

[1] Supported by the Council for Chemical Sciences, Dutch Organization of Scientific Research. Present address: Dept. of Microbiology and Molecular Medicine, Centre Médical Universitaire, CH-1211 Geneva, Switzerland.

[2] Supported by the Council for Earth and Life Sciences, Dutch Organization of Scientific Research. Present address: Dept. of Biochemistry, Biozentrum, University of Basel, CH-4056, Switzerland.

[3] To whom correspondence should be addressed. Tel.: 31-20-5987175; Fax: 31-20-5986979; E-mail: joen.luirink@falw.vu.nl.

[4] The abbreviations used are: PTC, peptidyl transferase center; TF, trigger factor; SRP, signal recognition particle; IMP, inner membrane protein; Ffh, fifty-four homologue; SA, signal anchor; TM, transmembrane segment; Lep, leader peptidase; SAKO, signal anchor knock-out; OMP, outer membrane protein.

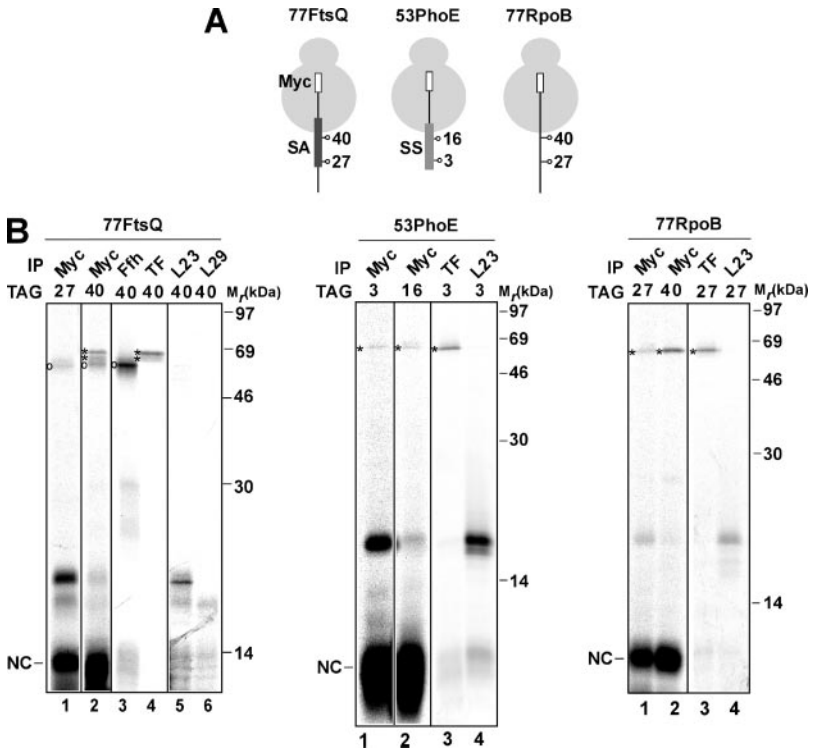

FIGURE 1. **Cross-linking of short nascent chains close to the ribosomal exit site.** *A*, schematic representation of nascent 77FtsQ, nascent 53PhoE, and nascent 77RpoB species. The signal anchor (*SA*), signal sequence (*SS*), and Myc epitope (*Myc*) are represented by a *dark*, a *gray*, and a *white bar*, respectively. The positions of the single photo cross-linking probes are indicated by a *stick-ball*. *B*, *in vitro* synthesis and cross-linking of nascent 77FtsQ, 53PhoE, and 77RpoB with single TAG codons in the coding sequence at indicated positions. After translation in the presence of (Tmd)Phe-tRNA^{sup}, samples were irradiated with UV light to induce photo cross-linking. The ribosome-nascent chain complexes (*RNCs*) were purified, immunoprecipitated (*IP*) as indicated, and analyzed by SDS-PAGE. Ffh adducts are indicated by an *open circle*, TF adducts are indicated by *asterisks*.

drop in contact at ~90 amino acids from the PTC. Strikingly, the SRP remained adjacent to emerging (hydrophilic) sequences downstream from the SA sequence and also contacted a second TM in a polytopic model protein.

EXPERIMENTAL PROCEDURES

Reagents and Sera—Restriction enzymes and the Expand long template PCR kit were purchased from Roche Applied Science. T4 DNA ligase was from Epicenter Technologies. Megashort T7 transcription kit was from Ambion Inc. [^{35}S]Methionine, protein A-Sepharose was from Amersham Biosciences. Sigma Chemicals Co. supplied all other chemicals. Antisera against L23/L29 and TF were kind gifts from R. Brimacombe and W. Wickner, respectively. Anti-Myc was from Sigma Chemicals Co. Antiserum against Ffh was from our laboratory collection.

Strains and Plasmids—Strain Top10F′ (Invitrogen) was used for routine maintenance of plasmid constructs. Strain MRE600 was used to obtain translation lysate for suppression of TAG stop codons in the presence of (Tmd)Phe-tRNA^{Sup} (30).

A C-terminal Myc epitope with amino acid sequence EQKLISEEDL was constructed downstream of the 4 methionines in the plasmid pC4Meth (31) resulting in the pMM plasmid (32). Plasmids encoding the various Lep nascent chains were described earlier (32). Plasmids encoding the various FtsQ proteins with single TAG codons were constructed in a two-step PCR procedure as follows: plasmids pMM77- to -168FtsQTAG40 were constructed by nested PCR using pC4Meth250FtsQTAG40 as a template (21).[5] Plasmid pMM77FtsQTAG27 was constructed by nested PCR using pC4Meth77FtsQTAG27 as a template (21). Plasmids pMM87FtsQTAG50, pMM97FtsQTAG60, pMM108FtsQTAG71, pMM128FtsQTAG91, pMM148FtsQTAG111, and pMM168FtsQTAG131 were constructed by nested PCR using pC4Meth250FtsQ as a template (21).[5]

[5] M. Urbanus and J. Luirink, unpublished data.

Plasmids encoding 128FtsQTAG40 and -TAG91 with a signal anchor knock-out (SAKO) mutation carried the substitutions L29R, L32R, and V38P. The mutations were introduced by site-directed mutagenesis resulting in pMM128FtsQTAG40SAKO and pMM128FtsQTAG91SAKO, respectively. Single TAG codons were introduced at positions 3 and 16 in 53PhoE using pC4Meth150PhoE as a template (33) in a nested PCR procedure resulting in pMM53PhoETAG3 and -TAG16, respectively. Single TAG codons were introduced at positions 27 and 40 in 77RpoB using pC4Meth150RpoB as a template (14) in a nested PCR procedure resulting in pMM77RpoBTAG27 and -TAG40, respectively. The nucleotide sequences of the mutant genes were confirmed by DNA sequencing.

In Vitro Transcription, Translation, and Cross-linking in S-135 Extract—Truncated mRNA was prepared as previously described (31) from the various ClaI-linearized pMMLep-, pMMFtsQ-, pMMPhoE-, and pMMRpoB-derivative plasmids. *In vitro* translation was carried out in an *E. coli* cell- and membrane-free S-135 extract described previously (18). Photo cross-linking was carried out as described (31). Ribosome-nascent chain complexes were collected as described (21) and analyzed by SDS-PAGE after immunoprecipitation essentially as described (31). The labeled bands were quantified using the ImageQuant software (Amersham Biosciences) and corrected for translation efficiency of the Myc-tagged nascent chains as described (21, 32).

RESULTS

Model Proteins and Experimental Approach—Photo cross-linking was used to study sequential molecular contacts of nascent polypeptides of different nature with chaperones and targeting factors in the *E. coli* cytosol. Nascent chains of four model *E. coli* proteins were analyzed. First, FtsQ, an IMP involved in cell division, that has one TM and an N-in, C-out topology. Second, Leader peptidase (Lep), the major signal peptidase, an IMP with two TMs and an N-out, C-out topology. Third, PhoE, an outer membrane protein (OMP) synthesized with an N-terminal-cleaved signal peptide. Fourth, RpoB, the β-subunit of the RNA polymerase, a cytosolic protein. Both FtsQ and Lep are targeted via the

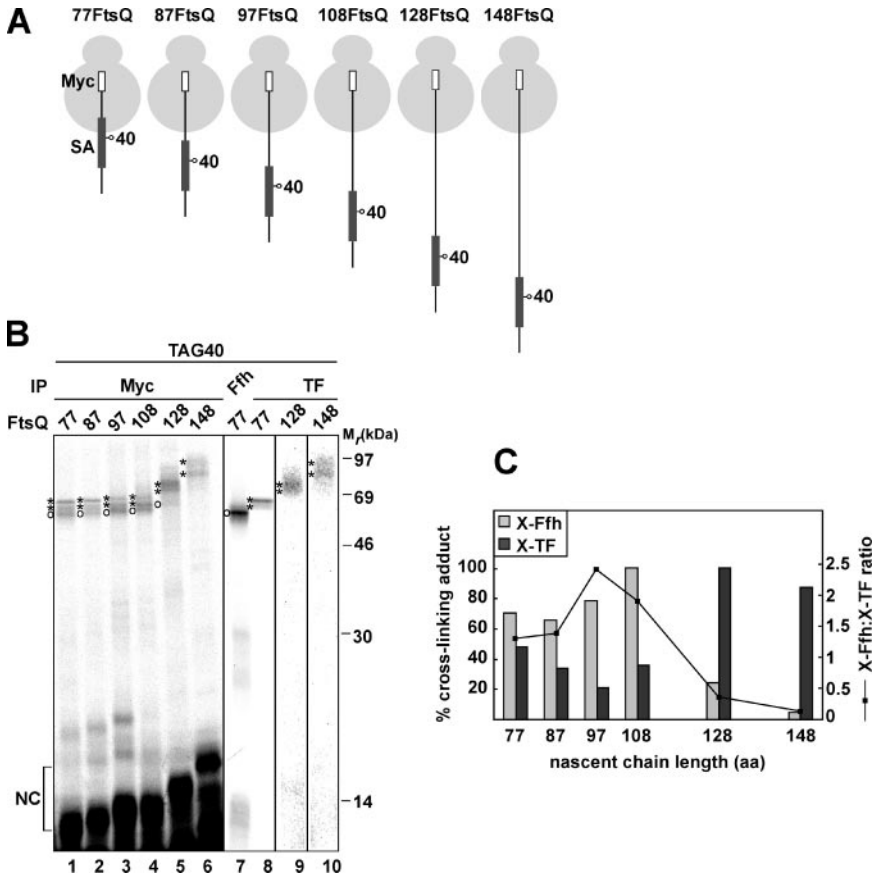

FIGURE 2. **Cross-linking of the FtsQ SA sequence upon elongation of the nascent chains.** *A*, schematic representation of nascent FtsQ chains with a single photo cross-linking probe at position 40 in the core of the SA sequence. *B*, *in vitro* synthesis, photo cross-linking, purification, and immunoprecipitation of nascent FtsQ 77–148mer, all with a single TAG codon at position 40 in the coding sequence. Ffh and TF adducts are indicated by an *open circle* and *asterisks*, respectively. *C*, Ffh and TF cross-linking adducts from *panel B*, *lanes 1–6*, were quantified and plotted as a histogram. The highest value for cross-linking efficiency was taken as 100%. The ratio of Ffh *versus* TF cross-linking (X-Ffh:X-TF ratio) per construct is depicted by a *graph*.

SRP-FtsY pathway to the Sec-YidC insertion site (34). PhoE is targeted by SecB to the Sec translocon (35).

Nascent chains of different length and nature were prepared by *in vitro* translation in a crude *E. coli* cell- and membrane-free extract in the presence of [^{35}S]methionine. Truncated mRNAs were used that include a C-terminal sequence encoding 4 methionines to increase the labeling efficiency and a Myc epitope to allow selective immunopurification of nascent chains that have reached the proper length. We have recently shown that the use of this Myc tag is essential to eliminate aberrant shorter translation products and their cross-linked partners (32).

To enable site-directed photo cross-linking, a TAG (stop) codon was introduced at indicated positions. The TAG codon was suppressed during translation by adding a suppressor tRNA that carries a phenylalanine coupled to a photoreactive cross-linking (Tmd) probe (see "Experimental Procedures"). In all constructs, the TAG mutation was efficiently suppressed by the (Tmd)Phe-tRNA^{sup}, resulting in nascent chains of the expected molecular weight (not shown). After translation, the probe was activated by UV irradiation to covalently link nascent chains to any molecules that are in close proximity. Subsequently, the samples were immunoprecipitated and analyzed by SDS-PAGE and phosphorimaging, resulting in characteristic and reproducible cross-linking patterns. As a note of caution, it should be pointed out that partial folding of nascent chains might take place in the ribosome, which could influence the precise distance between the PTC and the cross-linking probe (22, 36).

The Nature of the Exposed Nascent Chain Is Critical for Contact with Ffh—We have previously shown that nascent FtsQ with a length of 77 amino acids is the shortest translation intermediate that efficiently inserts into the membrane, as judged by the criterion of carbonate resistance and cross-linking to SecY (18). At this length the majority of the TM is exposed outside the ribosome (Fig. 1*A*). Scanning photo cross-linking indicates that in the absence of membranes the TM in 77FtsQ contacts Ffh from most positions, consistent with a role of the SRP in targeting of FtsQ (21). In addition, cross-linking to TF and the ribosomal proteins L23 and L29 has been observed (21).

To investigate whether these early interactions depend on the nature and future destination of the nascent polypeptide we have compared the earliest interactions of the IMP FtsQ, the OMP PhoE, and the cytosolic protein RpoB. Interactions were probed by photo cross-linking from positions in the Myc-tagged constructs that are located 37 and 50 amino acids from the PTC. We analyzed 77FtsQ, 77RpoB, and 53PhoE (Fig. 1*A*). 53PhoE was chosen to bring the same spacing between the PTC and the PhoE signal peptide as between the PTC and the TM in 77FtsQ. 77FtsQTAG27 and -TAG40 were cross-linked and immunoprecipitated using antibodies against the Myc epitope (Fig. 1*B*, *left panel*, *lanes 1* and *2*). Cross-linking to Ffh, TF, L23, and L29 in these samples was confirmed by separate immunoprecipitations (Fig. 1*B*, *left panel*, *lanes 3–6*, and data not shown). These results confirm earlier data (21) using untagged nascent chains suggesting that the Myc tag at the C terminus of nascent FtsQ does not influence contacts of the TM outside the ribosome, contacts that apparently do not derive from premature pausing products. As observed earlier, the TF adducts migrate as a doublet (16, 21, 25).

Similar analysis of 53PhoE and 77RpoB demonstrated that both constructs are cross-linked to TF and L23 from both positions in the nascent chain, but not to Ffh (Fig. 1*B*, *middle* and *right panels*, and data not shown). Notably, in the wild-type translation extract used, the TF:SRP ratio is similar to that in living cells, *i.e.* ~300:1 (Refs. 8, 37, and data not shown). This suggests that the substrate specificity of the SRP is determined at this early stage by the nature of the peptide that is exposed

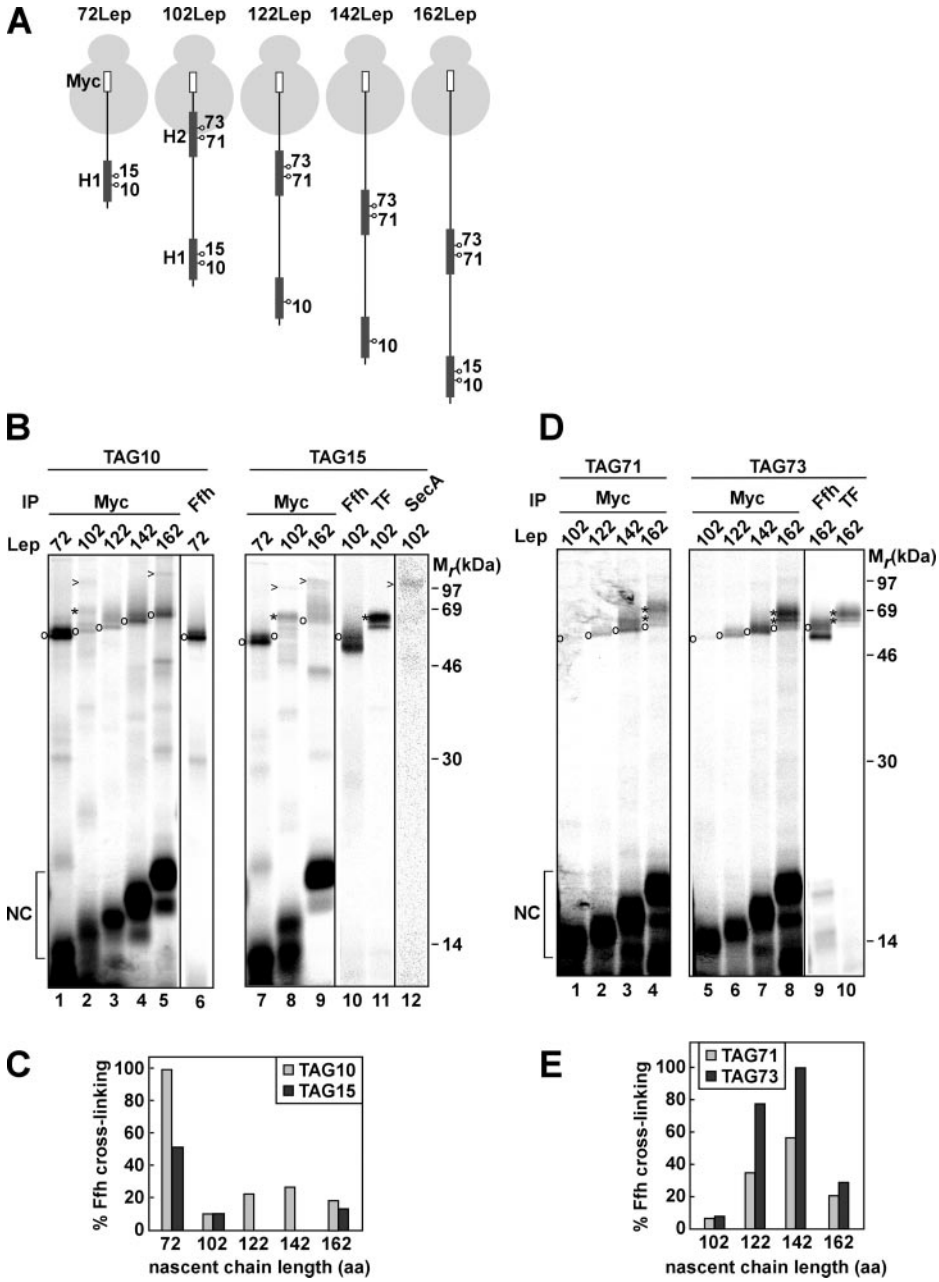

FIGURE 3. **Lep H1 and H2 are both efficiently cross-linked to Ffh.** *A*, schematic representation of nascent Lep chains with single photo cross-linking probes at indicated positions in H1 and H2. *B* and *D*, *in vitro* synthesis, photo cross-linking, purification, and immunoprecipitation of nascent Lep (sizes indicated) with a single TAG codon at position 10 (*panel B*, *lanes 1–6*), 15 (*panel B*, *lanes 7–12*), 71 (*panel D*, *lanes 1–4*), or 73 (*panel D*, *lanes 5–10*) in the coding sequence. Ffh and TF adducts are indicated by an *open circle* and *asterisk*, respectively. SecA adducts are indicated by a right-pointing angle. *C* and *E*, Ffh cross-linking adducts from *panel B*, *lanes 1–5*, *7–9* (*C*) and from *panel D*, *lanes 1–4*, *5–8* (*E*) were quantified. The highest value for cross-linking efficiency was taken as 100%.

close to the exit site. Importantly, even in elongation-arrested nascent chains, the SRP appears capable of discriminating between a signal peptide of a secreted protein and a future TM of an IMP. In all three constructs, cross-linking to L23 is more pronounced from position 50 (relative to the PTC) than from position 37, suggesting that the N terminus of the nascent chain remains sequestered near the surface of the ribosome at this stage in translation (see below).

Co-translational Interaction of Ffh with a Nascent IMP Depends on Nascent Chain Length—What happens to these early cytosolic contacts of a TM during nascent chain elongation? To investigate this, we lengthened the FtsQ nascent chains with a cross-link probe at position 40 in the TM up to 148 amino acids (Fig. 2*A*). The relative efficiency of Ffh cross-linking as compared with TF cross-linking peaked at 97 amino acids (cross-link probe 57 residues from the PTC; Fig. 2, *B* and *C*). Cross-linking to Ffh was efficient up to 108 amino acids (cross-link probe 68 residues from the PTC) but dropped sharply using the 128- and 148FtsQ constructs (cross-link probe 88 respectively 108 residues from the PTC), which, instead, showed more efficient cross-linking to TF (Fig. 2, *B* and *C*). Cross-linking to L23 was not readily detectable in constructs longer than 97 residues.

To study whether this length dependence of TM contacts is generic, we used Lep constructs of 72 to 162 amino acids with cross-link probes at position 10 or 15 in the first TM (Fig. 3*A*). Previous studies have already shown that 50Lep contacts Ffh and is targeted to the Sec translocon similar to 77FtsQ (19, 22).

Clearly, 72Lep is most efficiently cross-linked to Ffh from both positions in H1 (Fig. 3*B*, *lanes 1*, *6*, *7*, and Fig. 3*C*). At this length, the distance of the cross-link probes in H1 to the PTC site is ~60 amino acid residues. Similarly, 108FtsQ, with a distance of 68 amino acids between the probe in the TM and the PTC (Fig. 1*A*), was most efficiently cross-linked to Ffh (Fig. 2*C*).

Nascent Lep of 102 amino acids with H1 well exposed outside the ribosome (cross-link probes ~90 residues from the PTC) showed cross-linking to Ffh, TF, and SecA from both positions (Fig. 3*B*, *lanes 2*, *8*,

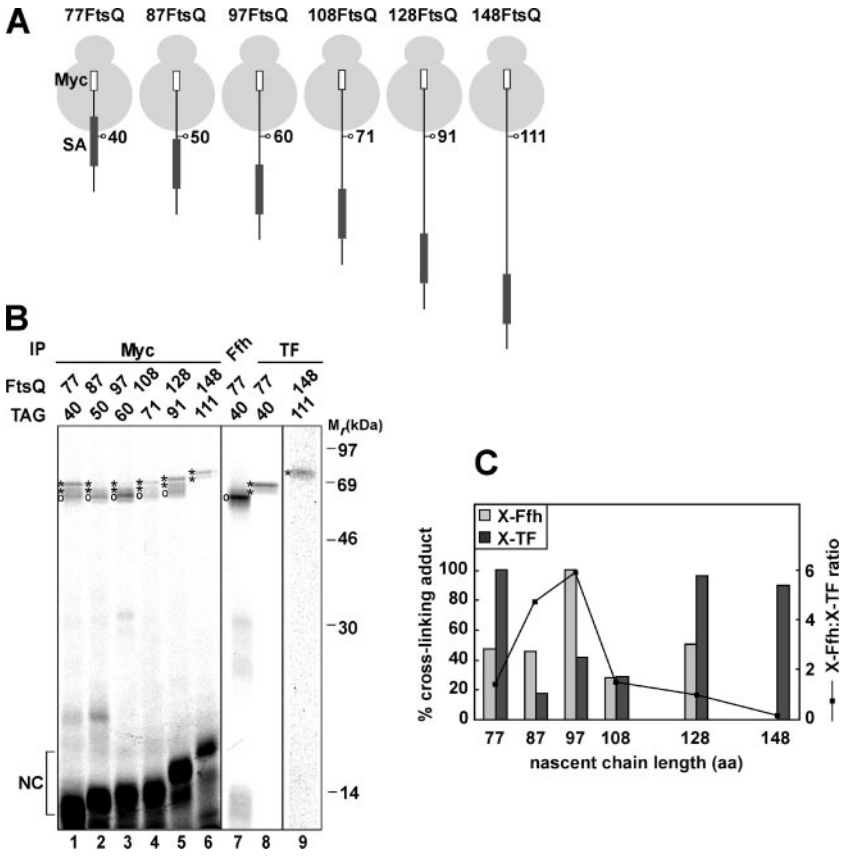

FIGURE 4. **The molecular environment of nascent FtsQ chains near the ribosome exit site upon elongation.** *A*, schematic representation of nascent FtsQ chains with single photo cross-linking probe at the indicated positions, close to the ribosomal exit region. *B*, *in vitro* synthesis, photo cross-linking, purification, and immunoprecipitation of nascent FtsQ (sizes indicated). Ffh and TF adducts are indicated by an *open circle* and *asterisks*, respectively. *C*, TF and Ffh cross-linking adducts from *panel B*, *lanes 1–6*, were quantified and plotted as a histogram. The highest value for cross-linking efficiency was taken as 100%. The ratio of Ffh *versus* TF cross-linking (X-Ffh:X-TF ratio) per construct is depicted by a *graph*.

10–12, and 3*C*), suggesting a somewhat flexible orientation near the ribosome exit site. Notably, compared with 72Lep, the efficiency of cross-linking to Ffh dropped dramatically in 102Lep, again similar to the cross-link results with the comparable FtsQ construct (128FtsQ; Fig. 2*C*). SecA is known to be required only at a later stage in the biogenesis of Lep (38). When the nascent chain in 102Lep is fully extended, H2 is expected to be partly exposed (Fig. 3*A*), which prompted us to investigate its molecular contacts. Cross-linking to H2 was probed from positions 71 and 73 near the center of the TM. Surprisingly, H2 cross-linked Ffh from both positions, albeit weakly (Fig. 3*D*, *lanes 1* and *5*, and 3*E*). Apparently, H2, which is almost as hydrophobic as H1, can also be recognized as a targeting signal at this stage.

In the longer constructs (122-, 142-, and 162Lep) cross-linking of H1 to Ffh was still detected. Additionally, SecA was cross-linked to 162Lep from both positions 10 and 15. H2 in 122- and 142Lep showed exclusive and optimal Ffh cross-linking from both positions 71 and 73 (Fig. 3*D*, *lanes 2*, *3*, *6*, *7*, and 3*E*). In these constructs the cross-link probes are ~50–70 residues from the PTC. In 162Lep (cross-link probes ~90 residues from the PTC), Ffh cross-linking to H2 dropped and was replaced by TF. Cross-linking to L23 was not detected in these longer constructs.

Together, the data suggest that Ffh is close to the TMs in FtsQ and Lep immediately when they emerge from the ribosome near L23, with optimal contact at ~50–70 amino acids from the PTC and a sharp drop in contact at ~90 amino acids from the PTC. TF is close to all TMs with no apparent preference for nascent chain length, but its proximity is competed by Ffh. Consequently, TF contacts become more apparent when contact with Ffh is lost.

Ffh Remains Adjacent to the Ribosome Exit Site during Elongation of FtsQ—77FtsQTAG40 is the shortest translation intermediate that contacts both Ffh and TF (21). In this construct the cross-link probe is in the TM, 37 amino acids from the PTC. We next probed the environment of nascent FtsQ near the exit site upon elongation. 77–148FtsQ constructs were analyzed with a cross-link probe at a constant distance of 37 amino acids from the PTC (Fig. 4*A*). Surprisingly, Ffh remained cross-linked until 128FtsQ, peaking in intensity at 97FtsQ (Fig. 4*B*, *lanes 1–5*, *7*, and 4*C*). In the longer construct contact with Ffh was lost and replaced by TF (Fig. 4*B*, *lanes 6* and *9*, and 4*C*). Thus, the relative cross-linking efficiencies of Ffh and TF to the TM (Fig. 2*C*) and to the downstream hydrophilic sequence (Fig. 4*C*) coincide, suggesting that Ffh initially tethers the growing FtsQ to the ribosome.

We next investigated to what extent the molecular contacts near the exit site are dictated by a functional TM in the upstream sequence. The nascent 128FtsQTAG40 and TAG91 constructs were modified in the TM by replacing three apolar amino acids by two basic amino acids and one proline residue (see Fig. 5*A*). The resulting SAKO mutants failed to be targeted to the inner membrane, arguing that the TM was effectively disrupted, as expected (data not shown). Upon UV irradiation 128FtsQTAG40-SAKO was strongly cross-linked to TF, whereas Ffh adducts were not detected (Fig. 5*C*, *lane 2*). Apparently, the modified TM is too polar to be recognized by Ffh and is now free to interact more efficiently with TF in a seemingly default mechanism. Likewise, 128FtsQTAG91-SAKO is exclusively cross-linked to TF (Fig. 5*C*, *lane 4*), arguing that no Ffh is present at, or oriented toward, the nascent chain exit site. Taken together, the data indicate that the cross-linking of Ffh to photoprobes located in the hydrophilic part of longer nascent FtsQ near the ribosome exit site was only due to the interaction of Ffh with the upstream hydrophobic TM.

DISCUSSION

The present site-specific cross-link data suggest that the chaperone TF is adjacent to nascent polypeptides that protrude from the ribosomal tunnel by default. In contrast, Ffh, subunit of the SRP-targeting complex, specifi-

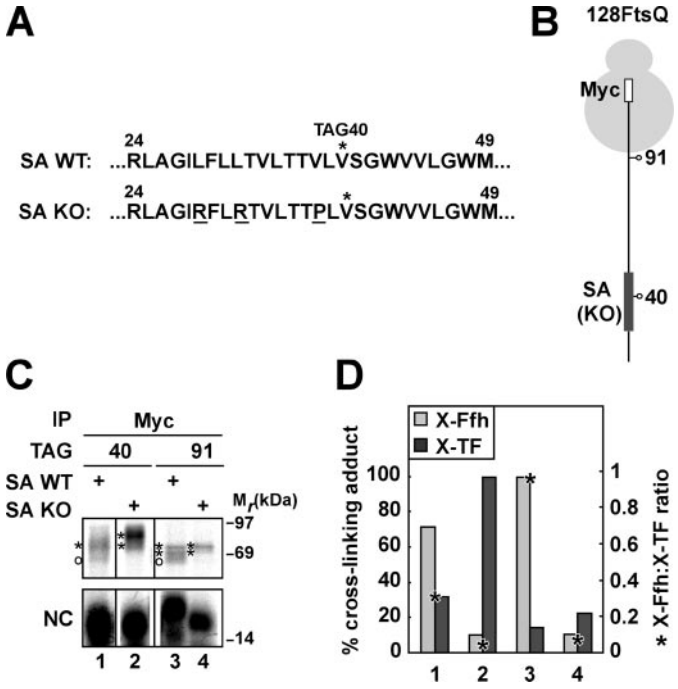

FIGURE 5. **Cross-linking near the exit site is dictated by a functional SA sequence in the upstream region.** *A*, sequence of the wild-type (*SA WT*) and the mutant SA sequence (*SA KO*) of FtsQ. Substitutions in the SAKO variant are *underlined*. The cross-link probe at position 40 (TAG40) is indicated by an *asterisk*. *B*, schematic representation of 128FtsQ containing SA WT or SA KO sequence with a single photo cross-linking probe at the indicated position. *C*, *in vitro* synthesis, photo cross-linking, purification, and immunoprecipitation of nascent 128FtsQ species. Ffh and TF adducts are indicated by an *open circle* and *asterisks*, respectively. Only relevant gel regions are shown. *NC*, nascent chains. *D*, Ffh and TF cross-linking adducts from *panel C*, *lanes 1–4*, were quantified and plotted as a histogram. The highest value for cross-linking efficiency was taken as 100%. The ratio of Ffh *versus* TF cross-linking (X-Ffh:X-TF ratio) per construct is depicted by *asterisks*.

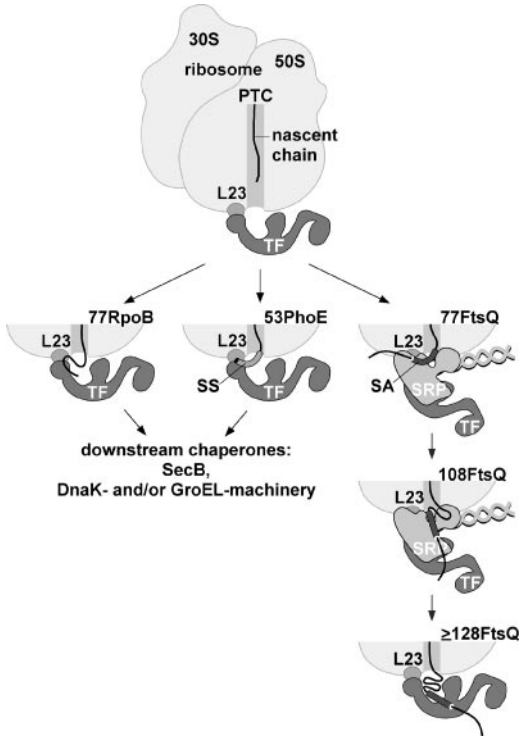

FIGURE 6. **Model for the first contacts of nascent polypeptides in the *E. coli* cytosol.** The *upper scheme* represents the ribosome, comprising the 30S and 50S subunits. The polypeptide exit tunnel located in the large ribosomal subunit is shown in *dark gray*. A nascent chain is represented by a *black solid line* and is positioned inside the tunnel starting from the PTC. At the exit region of the tunnel the ribosomal protein L23 is depicted in *dark gray*. The schemes below represent the bottom part of the 50S subunit where the nascent chain leaves the ribosome. TF binds L23 and arches over the exit site. SRP also associates with L23, sometimes simultaneously with TF. SRP is shown here in *light gray*, comprising Ffh and 4.5 S RNA (*coiled strand*). An α-helical signal sequence (*SS*) is shown as a *light-colored cylinder* and an α-helical signal anchor (*SA*) sequence as a *dark-colored cylinder*. The model is described under "Dicussion."

cally interacts with nascent IMPs, but not with nascent secretory proteins, effectively contending TF. Thus, IMPs are selected for co-translational targeting by the SRP at an early stage during biogenesis.

Both TF and SRP connect to the ribosome via L23 that is close to the exiting nascent chain (16, 21, 24, 26). When contacts in short nascent chains were probed from positions that are presumably close to this exit site (37 and 50 amino acids from the PTC), distinct cross-link patterns were observed depending on whether the nascent chain was derived from a cytosolic protein, an OMP, or an IMP (Fig. 1; model in Fig. 6). 77RpoB (cytosolic) and 53PhoE (OMP) were exclusively cross-linked to L23 and TF from both positions. Notably, in 53PhoE both probes are located in the signal sequence. In contrast, 77FtsQ is also cross-linked to Ffh from both position 40 (37 amino acids from the PTC), which is located in the core of the SA sequence, and position 27 (50 amino acids from the PTC). Using comparable constructs, another nascent IMP, Lep, is also cross-linked to Ffh (22). Strikingly, the N-terminal probe of all nascent chains is much stronger cross-linked to L23 than the C-terminal probe, indicating that the nascent chain exits the ribosome in a looped conformation with the N terminus tethered near L23.

Our findings contrast with data obtained by Müller and co-workers (25), who observed cross-linking of Ffh, but not of TF, to the signal peptide of nascent OmpA of similar length. Like PhoE, OmpA is a SecB-dependent outer membrane protein that should not contact Ffh at any stage during biosynthesis to avoid overload of the co-translational targeting pathway that is primarily reserved for IMPs. The reason for the discrepancy in the results might stem from a difference in translation system. We use a crude S-135 extract, whereas the Müller group uses a semi-purified extract with addition of purified targeting factors and chaperones. The latter system does not contain the normal ratio of cytosolic components that might influence the delicate balance of nascent chain interactions. In the crude lysate used in this study, Ffh appears perfectly able to select the appropriate substrates for co-translational targeting immediately upon emergence of a sequence of sufficient hydrophobicity. Consistently, SRP has been shown to effectively compete the proximity of TF to nascent FtsQ in a semi-reconstituted translation system (21).

It remains unclear at which stage and by what mechanism the SRP is recruited at the nascent exit site during biogenesis of an IMP. The low cellular abundance of the SRP (37) precludes a permanent residence near each exit site to scan emerging peptides for strongly hydrophobic targeting signals. It has been suggested that the ribosome itself may sense passing sequences and respond by recruiting chaperones, targeting factors, and translocon components near the exit site (6, 36, 39). However, we have no evidence for an intra-ribosomal signaling mechanism by which a TM in the exit tunnel recruits the SRP near the exit site (22). Rather, we are inclined to believe that the *E. coli* Ffh, like its eukaryotic counterpart (40), binds rapidly to the emerging TM by virtue of its exceptionally high affinity for ribosome-nascent-chain complexes with an exposed TM (Fig. 6). Most likely, TF, if associated with L23 at this stage, must undergo a substantial change in conformation and orientation to allow the SRP to access the nascent IMP (29). In any case, Ffh cross-linking from a crude translation lysate appears a useful tool to predict SRP-mediated targeting.

Ffh cross-linking to the nascent IMP is most efficient when the SA sequence is ~50–70 amino acids from the PTC, with a sharp drop in

efficiency at ~90 amino acids from the PTC (Figs. 2 and 3; model in Fig. 6). This implies a short time window for successful co-translational targeting unless the SRP has translation arrest activity *in vivo*, a function that is still controversial for the *E. coli* SRP (discussed in Ref. 7) but also for the eukaryotic SRP (40). The *E. coli* SRP appears to remain juxtaposed to the nascent chain exit site after passage of the SA sequence as judged from its cross-linking to protruding sequences downstream from the SA probed from a constant distance of 37 amino acids from the PTC (Fig. 4; model in Fig. 6). This suggests a looped conformation in which the SA is transiently sequestered near the exit site by the SRP, consistent with the cross-linking to L23. Upon further elongation, both the SA (now >90 residues from the PTC) and downstream sequences lose contact with SRP to the benefit of TF (Fig. 6). Most likely, the SRP is released from the ribosome at this stage, giving room to TF unless a second TM of sufficient hydrophobicity comes along. The arched structure of TF (17) may accommodate relatively large protein domains and explain the observed links with longer nascent chains that have also been observed before (41). Upon completion of synthesis, IMPs that have failed to contact SRP will be abandoned by TF as well. These orphan IMPs in the cytosol will be eliminated by quality control mechanisms as they are potentially toxic due to their hydrophobic, aggregation-prone nature (42).

In some of the longer Lep constructs cross-linking to SecA was detected. SecA is known to be involved in the post-translational targeting of secretory proteins (reviewed in Ref. 43). However, its affinity for targeting sequences (44) and the ribosome (45) may point to an additional role in co-translational targeting.

Relatively long elongation-arrested nascent chains of Lep were shown to associate with Ffh via their second TM as well (Fig. 4). Thus, in polytopic IMPs, a subsequent TM may provide an additional chance for SRP-mediated targeting as demonstrated for polytopic endoplasmic reticulum membrane proteins (46, 47). Whether this contact is relevant *in vivo* for co-translational membrane targeting and subsequent assembly of Lep remains to be determined.

Acknowledgments—We thank Corinne ten Hagen-Jongman for technical support and J.-W. de Gier, D.-J. Scheffers, W. Jong, and P. Genevaux for critical reading of the manuscript.

REFERENCES

1. Nissen, P., Hansen, J., Ban, N., Moore, P. B., and Steitz, T. A. (2000) *Science* **289,** 920–930
2. Harms, J., Schluenzen, F., Zarivach, R., Bashan, A., Gat, S., Agmon, I., Bartels, H., Franceschi, F., and Yonath, A. (2001) *Cell* **107,** 679–688
3. Etchells, S. A., and Hartl, F. U. (2004) *Nat. Struct. Mol. Biol.* **11,** 391–392
4. Young, J. C., Agashe, V. R., Siegers, K., and Hartl, F. U. (2004) *Nat. Rev. Mol. Cell. Biol.* **5,** 781–791
5. Craig, E. A., Eisenman, H. C., and Hundley, H. A. (2003) *Curr. Opin. Microbiol.* **6,** 157–162
6. Albanese, V., and Frydman, J. (2002) *Nat. Struct. Biol.* **9,** 716–718
7. Luirink, J., and Sinning, I. (2004) *Biochim. Biophys. Acta* **1694,** 17–35
8. Lill, R., Crooke, E., Guthrie, B., and Wickner, W. (1988) *Cell* **54,** 1013–1018
9. Stoller, G., Rucknagel, K. P., Nierhaus, K. H., Schmid, F. X., Fischer, G., and Rahfeld, J. U. (1995) *EMBO J.* **14,** 4939–4948
10. Genevaux, P., Keppel, F., Schwager, F., Langendijk-Genevaux, P. S., Hartl, F. U., and Georgopoulos, C. (2004) *EMBO Rep.* **5,** 195–200
11. Kramer, G., Patzelt, H., Rauch, T., Kurz, T. A., Vorderwulbecke, S., Bukau, B., and Deuerling, E. (2004) *J. Biol. Chem.* **279,** 14165–14170
12. Teter, S. A., Houry, W. A., Ang, D., Tradler, T., Rockabrand, D., Fischer, G., Blum, P., Georgopoulos, C., and Hartl, F. U. (1999) *Cell* **97,** 755–765
13. Deuerling, E., Schulze-Specking, A., Tomoyasu, T., Mogk, A., and Bukau, B. (1999) *Nature* **400,** 693–696
14. Ullers, R. S., Luirink, J., Harms, N., Schwager, F., Georgopoulos, C., and Genevaux, P. (2004) *Proc. Natl. Acad. Sci. U. S. A.* **101,** 7583–7588
15. Ying, B. W., Taguchi, H., Kondo, M., and Ueda, T. (2005) *J. Biol. Chem.* **280,** 12035–12040
16. Kramer, G., Rauch, T., Rist, W., Vorderwulbecke, S., Patzelt, H., Schulze-Specking, A., Ban, N., Deuerling, E., and Bukau, B. (2002) *Nature* **419,** 171–174
17. Ferbitz, L., Maier, T., Patzelt, H., Bukau, B., Deuerling, E., and Ban, N. (2004) *Nature* **431,** 590–596
18. Urbanus, M. L., Scotti, P. A., Froderberg, L., Saaf, A., de Gier, J. W., Brunner, J., Samuelson, J. C., Dalbey, R. E., Oudega, B., and Luirink, J. (2001) *EMBO Rep.* **2,** 524–529
19. Houben, E. N., Urbanus, M. L., van der Laan, M., ten Hagen-Jongman, C. M., Driessen, A. J., Brunner, J., Oudega, B., and Luirink, J. (2002) *J. Biol. Chem.* **277,** 35880–35886
20. Beck, K., Eisner, G., Trescher, D., Dalbey, R. E., Brunner, J., and Muller, M. (2001) *EMBO Rep.* **2,** 709–714
21. Ullers, R. S., Houben, E. N., Raine, A., ten Hagen-Jongman, C. M., Ehrenberg, M., Brunner, J., Oudega, B., Harms, N., and Luirink, J. (2003) *J. Cell Biol.* **161,** 679–684
22. Houben, E. N., Zarivach, R., Oudega, B., and Luirink, J. (2005) *J. Cell Biol.* **170,** 27–35
23. Pool, M. R., Stumm, J., Fulga, T. A., Sinning, I., and Dobberstein, B. (2002) *Science* **297,** 1345–1348
24. Gu, S. Q., Peske, F., Wieden, H. J., Rodnina, M. V., and Wintermeyer, W. (2003) *RNA* **9,** 566–573
25. Eisner, G., Koch, H. G., Beck, K., Brunner, J., and Muller, M. (2003) *J. Cell Biol.* **163,** 35–44
26. Buskiewicz, I., Deuerling, E., Gu, S. Q., Jockel, J., Rodnina, M. V., Bukau, B., and Wintermeyer, W. (2004) *Proc. Natl. Acad. Sci. U. S. A.* **101,** 7902–7906
27. Raine, A., Ivanova, N., Wikberg, J. E., and Ehrenberg, M. (2004) *Biochimie (Paris)* **86,** 495–500
28. Halic, M., Becker, T., Pool, M. R., Spahn, C. M., Grassucci, R. A., Frank, J., and Beckmann, R. (2004) *Nature* **427,** 808–814
29. Halic, M., and Beckmann, R. (2005) *Curr. Opin. Struct. Biol.* **15,** 116–125
30. Ellman, J., Mendel, D., Anthony-Cahill, S., Noren, C. J., and Schultz, P. G. (1991) *Methods Enzymol.* **202,** 301–336
31. Scotti, P. A., Urbanus, M. L., Brunner, J., de Gier, J. W., von Heijne, G., van der Does, C., Driessen, A. J., Oudega, B., and Luirink, J. (2000) *EMBO J.* **19,** 542–549
32. Houben, E. N., ten Hagen-Jongman, C. M., Brunner, J., Oudega, B., and Luirink, J. (2004) *EMBO Rep.* **5,** 970–975
33. Valent, Q. A., de Gier, J. W., von Heijne, G., Kendall, D. A., ten Hagen-Jongman, C. M., Oudega, B., and Luirink, J. (1997) *Mol. Microbiol.* **25,** 53–64
34. Dalbey, R. E., and Chen, M. (2004) *Biochim. Biophys. Acta* **1694,** 37–53
35. Kusters, R., de Vrije, T., Breukink, E., and de Kruijff, B. (1989) *J. Biol. Chem.* **264,** 20827–20830
36. Woolhead, C. A., McCormick, P. J., and Johnson, A. E. (2004) *Cell* **116,** 725–736
37. Jensen, C. G., and Pedersen, S. (1994) *J. Bacteriol.* **176,** 7148–7154
38. Lee, J. I., Kuhn, A., and Dalbey, R. E. (1992) *J. Biol. Chem.* **267,** 938–943
39. de Gier, J. W., and Luirink, J. (2003) *EMBO Rep.* **4,** 939–943
40. Flanagan, J. J., Chen, J. C., Miao, Y., Shao, Y., Lin, J., Bock, P. E., and Johnson, A. E. (2003) *J. Biol. Chem.* **278,** 18628–18637
41. Jong, W. S., ten Hagen-Jongman, C. M., Genevaux, P., Brunner, J., Oudega, B., and Luirink, J. (2004) *Eur. J. Biochem.* **271,** 4779–4787
42. Bernstein, H. D., and Hyndman, J. B. (2001) *J. Bacteriol.* **183,** 2187–2197
43. Vrontou, E., and Economou, A. (2004) *Biochim. Biophys. Acta* **1694,** 67–80
44. Kebir, M. O., and Kendall, D. A. (2002) *Biochemistry* **41,** 5573–5580
45. Liebke, H. H. (1987) *J. Bacteriol.* **169,** 1174–1181
46. Kuroiwa, T., Sakaguchi, M., Omura, T., and Mihara, K. (1996) *J. Biol. Chem.* **271,** 6423–6428
47. Lu, Y., Xiong, X., Helm, A., Kimani, K., Bragin, A., and Skach, W. R. (1998) *J. Biol. Chem.* **273,** 568–576